

BALLISTIC-ELECTRON-EMISSION MICROSCOPY OF STRAINED $\text{Si}_{1-x}\text{Ge}_x$ LAYERS

A. M. Milliken, L. D. Bell, S. J. Manion, W. J. Kaiser, R. W. Fathauer, and W. J. Pike

Center for Space Microelectronics Technology

Jet Propulsion Laboratory

California Institute of Technology

Pasadena, CA 91109

Ballistic-electron-emission microscopy has been used to investigate the effects of strain on $\text{Si}_{1-x}\text{Ge}_x$ alloys. Lifting of the degeneracy of the conduction-band minimum of SiGe due to lattice deformation has been directly measured by application of BEEM spectroscopy to Ag/Si structures. Experimental values for this conduction-band splitting agree well with calculations. In addition, an unexpected heterogeneity in the strain of the SiGe layer is introduced by deposition of Au. This effect, not observed with Ag, is attributed to species interdiffusion and has important implications for metal/semiconductor devices based on pseudomorphic SiGe/Si material systems.

PACS Numbers: 73.30.+y, 71.70.Ej, 61.16.X, 73.40.Ns

Strained-layer SiGe alloys are expected to play an increasing role in Si-based heteroepitaxy. The rapid decrease of bandgap with alloy fraction makes pseudomorphic SiGe/Si a promising candidate for heterostructure devices. Novel devices such as heterojunction bipolar transistors and long-wavelength infrared detectors have been fabricated based on the SiGe/Si materials system.¹ However, fundamental aspects of strained SiGe electronic structure have not been directly measured. This paper describes the application of ballistic-electron-emission microscopy (BEM) to a characterization of the effects of strain on SiGe.

Molecular-beam epitaxy (MBE) has been used to grow SiGe layers on Si substrates. As long as the SiGe layers are thinner than the critical thickness for the introduction of misfit dislocations, they remain fully strained and pseudomorphic with the underlying Si lattice. Since the unstrained SiGe lattice constant is slightly larger than that of Si, the pseudomorphic SiGe layer is under compressive strain in the plane of the layer, and tensile strain perpendicular to the layer. This distortion of the SiGe lattice modifies the band structure of the material.^{3,4} The light- and heavy-hole valence bands are split at the zone center. In addition, the silicon-like six-fold-degenerate conduction-band minimum is split by this strain into two sets of minima with differing energies. The energies of the four in-plane minima are lowered slightly, and the energies of the two out-of-plane minima are raised. The dependence of this conduction-band splitting on Ge alloy fraction has been calculated^{3,4}. A measurement of this splitting by electron-energy-loss spectroscopy has recently been reported⁵ for a thin SiGe quantum well layer.

BEM utilizes scanning tunneling microscopy⁶ (STM) to inject electrons into a heterostructure by vacuum tunneling from the STM tip. Most BEM experiments to date have been performed on metal/semiconductor heterostructures. By varying the tip-sample voltage, the energies of the electrons injected into the metal may be controlled, and a spectroscopy of transport may be performed. BEM has been used in the past to characterize Schottky barrier height^{7,8} (S1111) and carrier transport through metal/semiconductor structures⁹⁻¹². Additional

aspects of the conduction band structure have also been characterized. In the case of GaAs, the satellite minima at the Γ and X points have been directly observed using BFEEM¹. Observation of these minima in the BFEEM spectra is enabled by scattering during the electron transport process through the metal and across the metal/semiconductor interface, which widens the initially narrow angular distribution produced by tunneling. This provides a large fraction of the injected electrons with parallel momentum k_{\parallel} sufficient to couple into states in the semiconductor with non-zero k_{\parallel} , such as the Γ states (and the four off-axis X minima) in GaAs(100). In addition, BFEEM spectra of Au/Si(111) appear nearly identical to those obtained for Au/Si(100)¹³, again indicating a large degree of scattering in the Au or at the Au/Si interface.

The samples were grown by MBE using a Riber EVA 320 system. N-type (100) substrates doped at 0.1 Ω -cm were spin-cleaned¹⁴ and either intrinsic or n-Si buffer layers were grown on all samples. Samples were grown with nominally pseudomorphically strained (below the critical thickness for the introduction of misfit dislocations) intrinsic $\text{Si}_{1-x}\text{Ge}_x$ layers. The strained layers were 50 nm thick, with either $x=0.18$ or $x=0.25$. A third sample was grown with a nominally pseudomorphic intrinsic 50 nm Si layer on a nominally relaxed intrinsic 300 nm $\text{Si}_{0.75}\text{Ge}_{0.25}$ layer. All epitaxial layers were grown at 550°C.

Immediately after completion of growth, the wafers were spin-cleaned with 5% HF:ethanol and stored in a nitrogen-purged glove-box. 9 mm squares were diced in the glove-box, and each was spin-cleaned again prior to room-temperature deposition of the metal to complete the BFEEM sample. X-ray photoemission spectroscopy (XPS) was used to characterize the surface of a $\text{Si}_{0.75}\text{Ge}_{0.25}$ sample. One measurement was performed on the as-stored wafer 10 days after growth. A second sample was removed from the glove-box and placed on a hotplate in air at 220°C for 1 minute. Both samples were again spin-cleaned prior to the XPS measurement. In both cases, no oxide was detected. In addition, atomic percentage of Ge as determined by XPS ranged from 25% to 27%, in good agreement with the nominal fraction, indicating that oxidation

had not significantly altered the alloy fraction of the surface relative to the bulk.

BEEM measurements were performed in a nitrogen-purged glove-box, both at room temperature and at 77K. Due to the large leakage currents in some samples, 77K was necessary for acquisition of spectra with large signal-to-noise. other than a reproducible change in Schottky barrier height, BEEM spectral features did not depend on measurement temperature.

Au/SiGe/Si samples were fabricated for BEEM using $\text{Si}_{.82}\text{Ge}_{.18}$ and $\text{Si}_{.75}\text{Ge}_{.25}$ MBE layers, with evaporated Au layers 7.5 nm thick. Whereas Au/Si(100) BEEM spectra show a single threshold, which is fit well by a simple phase-space model¹, the Au/SiGe/Si BEEM spectra usually exhibited two thresholds. Just as in the case of GaAs, these two thresholds correspond to the onset of electron transmission into two sets of states in the SiGe layer. These states are comprised of the two sets of conduction-band minima which are split by strain. Unexpectedly, the energy difference of these two thresholds was found to vary from spectrum to spectrum in the range 0 -350 meV, with a roughly uniform distribution of splittings within this range. A BEEM spectrum representative of one of the larger values of this splitting is shown in Fig. 1 a. The two-threshold nature of the spectrum is apparent, with a separation in this case of 304mV. Derived values of the BEEM thresholds for the case of $\text{Si}_{.75}\text{Ge}_{.25}$, compiled from many different spectra measured at 77K, are plotted in Fig. 2. The thresholds for each spectrum are ordered according to the size of the splitting. The absolute values of the thresholds as a function of Ge fraction may then be compared to theory⁴, which is also shown in Fig 2. It is seen that there is good agreement with the expected energies of the conduction band minima as a function of strain, indicating that the observed variation in splitting maybe assigned to heterogeneous strain in the SiGe.

It is clear from the BEEM results that there is a large spatial variation in strain of the SiGe layer. This variation was observed for the $\text{Si}_{.82}\text{Ge}_{.18}$ samples as well. In both cases, the energy difference of the two BEEM thresholds varied from zero to more than twice the calculated value.

Several possibilities exist for the cause of this heterogeneity. A variation in alloy fraction of the SiGe layer would produce a corresponding variation in the strain of the layer. However, this interpretation would imply that areas in which no splitting was observed should correspond to areas where the Ge fraction and the strain were nearly zero. In order to test this premise, BEEM spectra which showed only a single threshold were compiled, and the average SBH was calculated for each alloy fraction. The results are shown in Fig. 1 b. It can be seen that there is a steady decrease in S1111 with nominal alloy fraction. If these spectra represented areas where the Ge fraction was nearly zero, a SBH which is independent of the nominal bulk alloy fraction would be expected. Additionally, convergent-beam diffraction measurements¹⁵ performed in a transmission electron microscope (TEM) indicate uniform strain, with values corresponding to alloy fractions which agree with those obtained from XPS.

A second possible mechanism is the presence of an intrinsic structural variation of the SiGe layer. Such a variation has been observed in the form of a periodic strain relaxation^{16,17}. This relaxation produces a corrugated surface, with enhanced strain in the troughs and reduced strain at the crests. This corrugation has been observed to have a period of a few hundred nm and an amplitude of several of nm, although these parameters depend on Ge fraction and layer thickness. However, the MBE growth temperature at which this corrugation was found to occur is higher than that used for the SiGe layers discussed here. In order to unambiguously ascertain the presence of such a relaxation, high-resolution cross-sectional TEM was performed on the Si_{0.82}Ge_{0.18} material. The results are shown in Fig. 3a. It can be seen that the SiGe surface is flat, with no evidence of a relaxation such as that observed in ref. 17.

Since characterization of the bare SiGe surface indicated a uniform pseudomorphic layer, the possibility that the Au produces a heterogeneity that is not present on the as-grown SiGe layer was investigated. Cross-sectional TEM performed on a completed Au/SiGe/Si structure confirms that this is the case. A representative image is shown in Fig. 3b. It is apparent that the SiGe

surface has been dramatically roughened by the Au deposition. This roughness appears with an amplitude on the order of 3 nm, and on a length scale of order 20 nm.

In order to compare the effect of another metal to that of Au, a series of samples was fabricated utilizing a metal bilayer consisting of 5 nm of Ag, capped by 5 nm of Au. The top Au layer was necessary to prevent oxidation of the Ag. The lower SBE produced by Ag, coupled with the somewhat large leakage current which was characteristic of all the metal/SiGe structures, required that all measurements on the Ag systems be performed at 77K. The results of BEEM spectroscopy of these samples are shown in Fig. 4. In contrast to the Au/SiGe case, BEEM measurements of the Ag/SiGe structures yielded values of conduction band splitting which were uniform and in good agreement with theory.⁴ TEM imaging of one such sample confirmed that, as expected, the SiGe roughening which occurred with Au was absent in the Ag case. One such image is shown in Fig. 3c. These results strongly indicate a correlation between the SiGe roughening and the variation in strain observed by BEEM.

To determine whether the strain heterogeneity observed with Au is specific to SiGe, MBE was used to grow a thick (300 nm) $\text{Si}_{.75}\text{Ge}_{.25}$ layer in excess the critical thickness for strain relaxation. A pseudomorphically strained Si layer 50 nm thick was then grown on the relaxed SiGe. In this case the in-plane conduction-band minima are raised in energy, and the out-of-plane minima are lowered, but the magnitude of the splitting is the same as for strained SiGe. Au was deposited to complete the sample. BEEM spectroscopy of these samples revealed a variation in strain splitting equivalent to that observed for Au on strained SiGe, with values of splitting ranging from 0 to about 350 meV. This indicates that a process similar to that present for Au on SiGe is operative in the case of strained Si.

The deposition of Au onto Si is known to produce a strong intermixing reaction, even at room temperature. Although most work has been done on Si(111), Au/Si(100) has also been

studied¹⁸. It has been shown that an intermixed layer may form at the interface, which can be several nanometers thick.¹⁹ This intermixed region can be non-uniform, depending on trace contamination remaining at the Au/Si interface¹⁹, and perhaps on Au crystallite orientation. In the case of strained Si or SiGe layers, the BEM results suggest that the heterogeneous roughening of the interface leads to local modifications in the strain present in the layers. "This may be due either to structural relaxation of the roughened interface, producing a non-uniform strain field¹⁷, or to injection of defects into the strained layer by Au/Si interdiffusion, locally relieving strain in the layer.

In conclusion, the conduction-band splitting of strained Si and SiGe has been directly measured using BEM spectroscopy. For the case of Ag on SiGe, the energy splitting is uniform, with values which agree well with calculations. Deposition of Au on SiGe, however, produces a large degree of spatial heterogeneity in the strain of the SiGe layer. This characteristic is also seen on strained Si, and appears to be due to the intermixing of Au and Si, leading to a roughened interface and heterogeneous strain,

The research described in this paper was performed by the Center for Space Microelectronics Technology, Jet Propulsion Laboratory, California Institute of Technology, and was jointly sponsored by the Office of Naval Research and the Ballistic Missile Defense Organization / Innovative Science and Technology Office through an agreement with the National Aeronautics and Space Administration (NASA).

REFERENCES

1. For a recent review of theoretical and experimental work, see S. C. Jain and W. Hayes, *Semicond. Sci. Technol.* **6**, 547 (1991).
2. W. J. Kaiser and I. D. Bell, *Phys. Rev. Lett.* **60**, 1406 (1988); I. D. Bell and W. J. Kaiser, *Phys. Rev. Lett.* **61**, 2368 (1988). For a more complete review of BHEM, see I. D. Bell, W. J. Kaiser, M. H. Hecht, and L. C. Davis, in *Scanning Tunneling Microscopy*, edited by J. A. Stroscio and W. J. Kaiser (Academic Press, San Diego, 1993), pp. 307-348.
3. R. People, *Phys. Rev. B* **32**, 1405 (1985).
4. Chris G. Van de Wane and Richard M. Martin, *Phys. Rev. B* **34**, 5621 (1986).
5. P. F. Batson and J. F. Morar, *Phys. Rev. Lett.* **71**, 609 (1993).
6. G. Binnig, H. Rohrer, Ch. Gerber, and E. Weibel, *Phys. Rev. Lett.* **49**, 57 (1982).
7. A. Fernandez, H. D. Hallen, T. Huang, R. A. Buhrman, and J. Silcox, *J. Vac. Sci. Technol. B* **9**, 590 (1991).
8. M. Prietsch and R. Ludeke, *Phys. Rev. Lett.* **66**, 2511 (1991).
9. L. D. Bell, M. H. Hecht, W. J. Kaiser, and L. C. Davis, *Phys. Rev. Lett.* **64**, 2679 (1990).
10. A. M. Milliken, S. J. Manion, W. J. Kaiser, L. D. Bell, and M. H. Hecht, *Phys. Rev. B* **46**, 12826 (1992).
11. R. Ludeke, *Phys. Rev. Lett.* **70**, 214 (1993).
12. A. Bauer, M. T. Cuberes, M. Prietsch, and G. Kaindl, *Phys. Rev. Lett.* **71**, 149 (1993).
13. L. J. Schowalter and E. Y. Lee, *Phys. Rev. B* **43**, 9308 (1991).
14. P. J. Grunthaner, F. J. Grunthaner, R. W. Fathauer, T. L. Lin, M. H. Hecht, L. D. Bell, W. J. Kaiser, F. D. Schowengerdt, and J. H. Mazur, *Thin Solid Films* **183**, 197 (1989).
15. W. T. Pike, L. M. Brown, R. A. A. Kubiak, S. M. Newstead, A. R. Powell, E. H. C. Parker, and T. E. Whall, *J. Cryst. Growth* **111**, 925 (1991).
16. A. G. Cullis, D. J. Robbins, A. J. Pidduck, and P. W. Smith, *J. Cryst. Growth* **123**, 333 (1992).

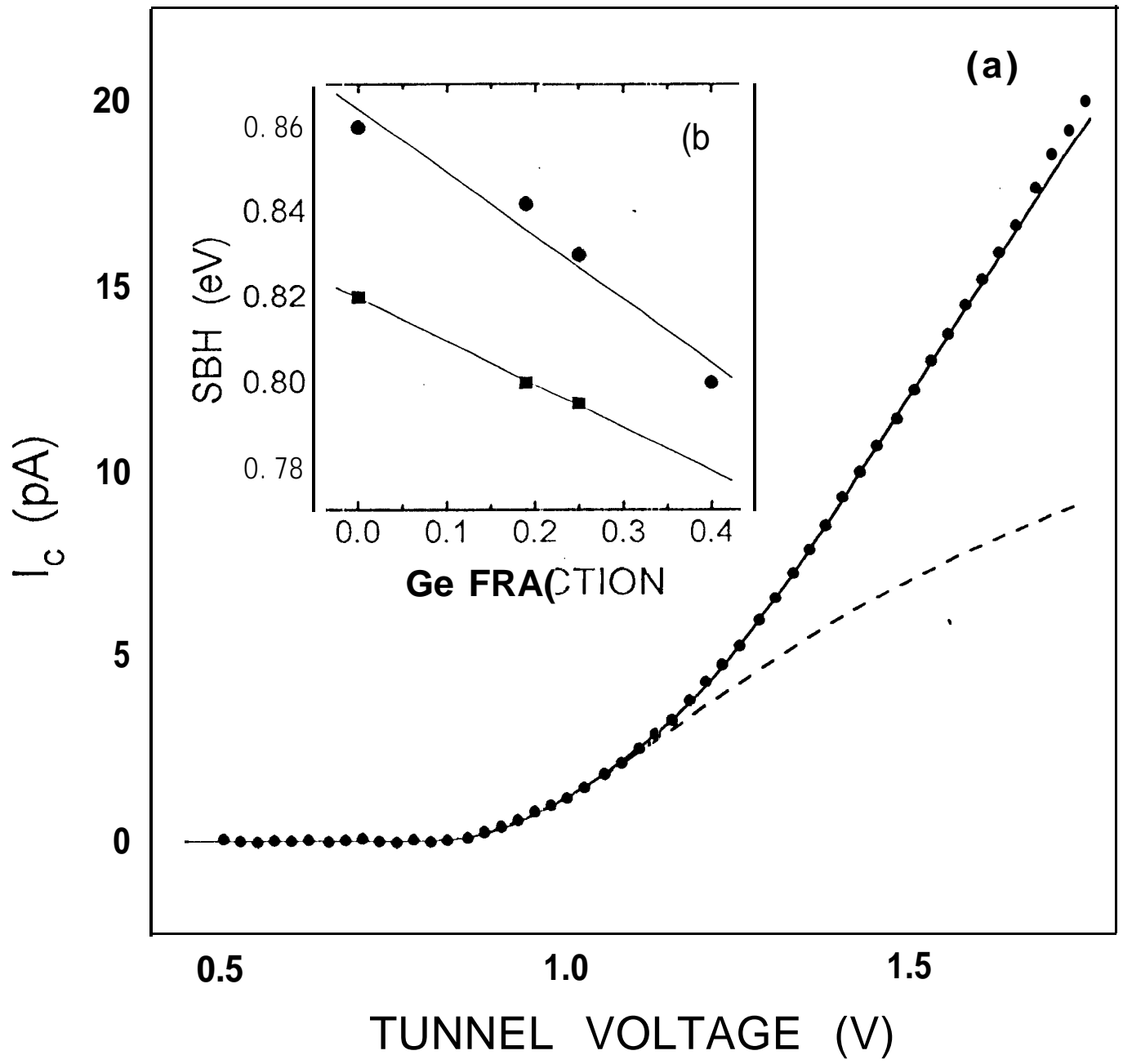
A. J. Pidduck, D. J. Robbins, A. G. Cullis, W. Y. Leong, and A. M. Pitt, *Thin Solid Films* 222, 78 (1992).

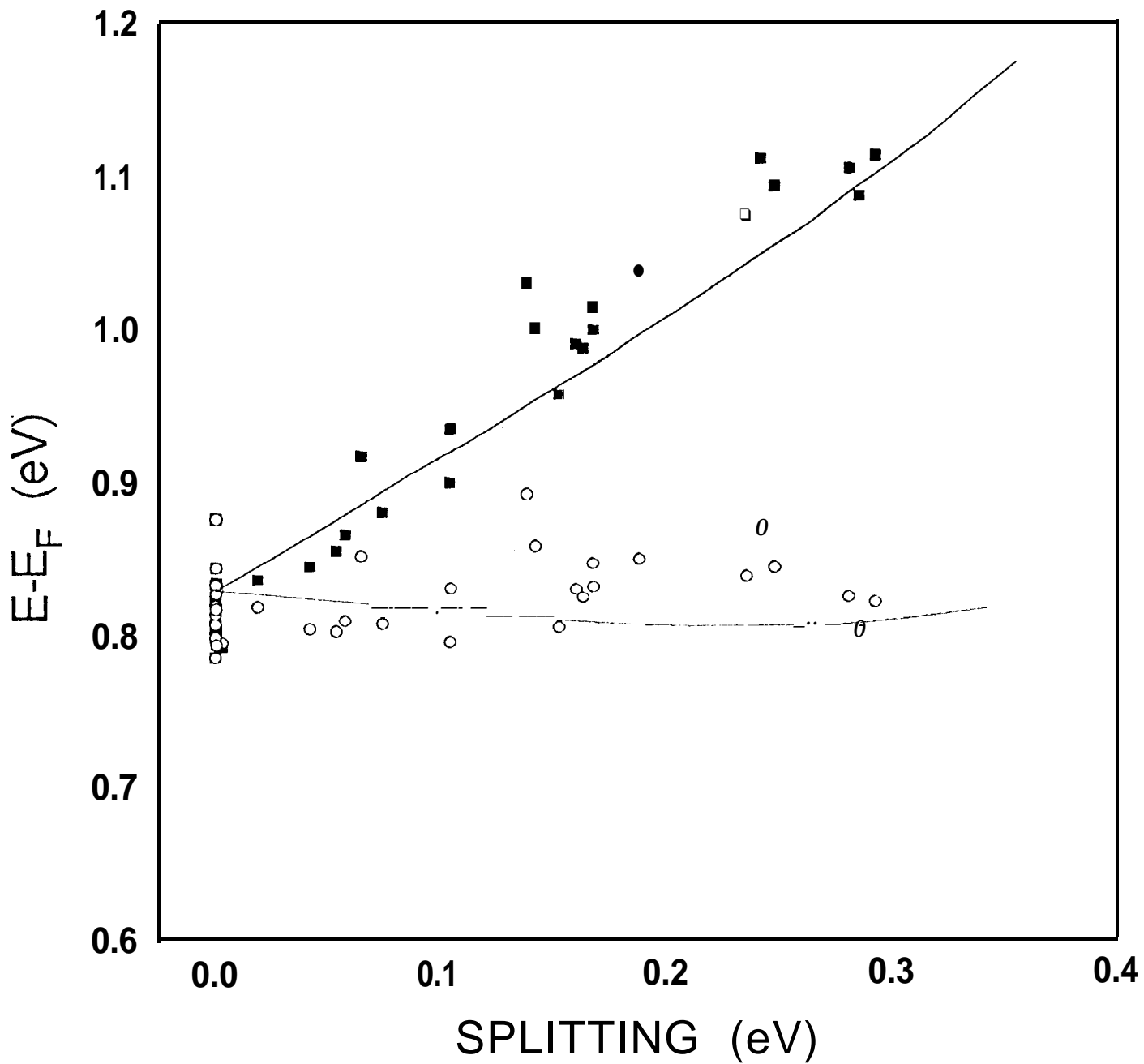
M. Hanbueken, Z. Imam, J. J. Metois, and G. Leelay, *Surf. Sci.* 162, 628 (1985).

Z. Ma and I. H. Allen, *Phys. Rev. B* 48, 15484 (1993).

FIGURES

1. (a) Experimental BEEM spectrum of collector current (I_c) versus tunnel voltage for a Au/Si_{0.75}Ge_{0.25}/Si(100) heterostructure. Tunnel current for this spectrum was 3 nA. The data are shown by circles. Also plotted are two theoretical spectra which have been fit to the data. The first (dashed line) fits only the low-voltage portion ($V < 1.1$ V) with a single threshold; the other fit (solid line) is over a larger range (to 1.6V) using a two-threshold model. The extracted thresholds for the two-threshold fit are separated by 304 mV. (b) Dependence of SBH on Ge fraction x , compiled from all Au/Si_{1-x}Ge_x/Si BEEM spectra showing only a single threshold. All individual spectra were fit to a two-threshold model, and the cases in which these thresholds converged to a single value are included here. Circles indicate 77K values, and squares indicate room temperature values. Also shown are best-fit lines to the data.
2. Plot of threshold values V_{b1} (open circles) and V_{b2} (solid squares) obtained from fitting all 77K data for Au/Si_{0.75}Ge_{0.25}/Si(100) samples, plotted versus splitting $V_{b1} - V_{b2}$. Also shown are theoretical curves (lines) from ref. 4.
3. High-resolution cross-sectional TEM images of Si_{1-x}Ge_x/Si structures. (a) Image of the as-grown Si_{0.75}Ge_{0.25}/Si material. (b) Image of a Si_{0.82}Ge_{0.18}/Si sample with an evaporated Au layer of nominal thickness 7.5nm. (c) Image of a Si_{0.82}Ge_{0.18}/Si sample with 5nm of evaporated Ag, capped with 5nm of Au.
4. Conduction-band splitting for Au/Ag/Si_{1-x}Ge_x/Si(100). The experimental points (circles) are derived from the fitted thresholds of the corresponding BEEM spectra. Also plotted (square) is the derived splitting for Au/Ag/Si/Si_{1-x}Ge_x(100) at $x=0.25$. The calculated dependence (line) is from ref. 4.







200 390KX 154591





